

Fabrication and dielectric properties of CCTO/PF dielectric composites: CCTO with different particle size

Yang Zhao^a, Yuzhen Zhao^a, Yuhua Niu^b, Yongming Zhang^a and Zongcheng Miao^{a,*}

^aKey Laboratory of Organic Polymer Photoelectric Materials, School of Science, Xijing University, Xi'an, 710123, Shaanxi, People's Republic of China

^bKey laboratory of Auxiliary Chemistry & Technology for Light Chemical Industry of Ministry of Education, Shaanxi University of Science & Technology, Xi'an, 710021, Shaanxi, People's Republic of China

Calcium copper titanate ($\text{CaCu}_3\text{Ti}_4\text{O}_{12}$, CCTO) particles with three types of particle size (CCTO-*i*, CCTO-*ii*, CCTO-*iii*) are prepared by wet chemical method. And then the dielectric composites based on CCTO particles and Phenol formaldehyde resin (PF) are fabricated by mixing and mould pressing. This paper mainly studies the microstructure and dielectric properties of CCTO/PF dielectric composites (CCTO-*i*, CCTO-*ii* and CCTO-*iii* composites). XRD, FTIR and SEM indicate that the CCTO particles are dispersed in the polymer matrix. In addition, the effect of particle size on the dielectric properties of CCTO/PF composites is also discussed. By comparing the CCTO/PF composites with different particle sizes, it is found that the CCTO-*i* composite has a high maximum dielectric constant and low loss at room temperature of 100 Hz, while the CCTO volume fraction was 0.5 in the measurement frequency range, which shows a very weak frequency dependence. On this basis, the CCTO-*i* composite with relatively small particle size has excellent dielectric properties, which may imply that the effect of interface will be changed by smaller particle size.

Keywords: CCTO particles, PF, Particle size, Dielectric property.

Introduction

In the past decades, ceramic/polymer dielectric composites exhibited high dielectric properties, good processability, owing to the combination of the advantage of the ceramic and polymer. The composite could be used in the fields of the high density capacitors, embedded microcapacitors, artificial muscles and so on. Recently, trends for these electronic devices require functionality, high-speed performance, miniaturization and lower cost. Therefore, developing new types of ceramic/polymer dielectric composites with relatively high dielectric properties to satisfy requirement of miniaturization and multifunctionality of electronic devices become an important subject in the area of the engineering and technology [1-7].

Currently, among the ceramic/polymer dielectric composites, the ceramics of BaTiO_3 (BT), $\text{Ba}_{0.6}\text{Sr}_{0.4}\text{TiO}_3$ (BST), $\text{Pb}(\text{Zr}, \text{Ti})\text{O}_3$ (PZT), and $\text{Pb}(\text{Mg}_{1/3}\text{Nb}_{2/3})\text{O}_3$ - PbTiO_3 (PMN-PT) exhibit relatively high dielectric permittivity [8-11]. These ceramics would be used as inorganic filler which mixed with the polymer matrix to form the ceramic/polymer dielectric composites. However, such ceramics always exhibit strong electro-

mechanical effects (such as piezoelectric effect), which limits the reliability of the devices [12, 13]. Recently $\text{CaCu}_3\text{Ti}_4\text{O}_{12}$ (CCTO) with environment friendly, giant permittivity, low loss tangent and better temperature stability is introduced as ceramic fillers to further increase the dielectric constant of the composites [14, 15]. What's more, Polyimide (PI), Poly (polyvinylidene-trifluoroethylene) (P(VDF-TrFE)), Epoxy resin, Silicone resin, Polyvinylidene fluoride (PVDF), and Polyaniline (PU), especially Phenol formaldehyde resin (PF) that exhibit high mechanical strength, good insulativity and heat resistance, are selected as polymer matrix [16-21]. To summarize, new types of CCTO/polymer composite have been investigated. Dang et al. [22] fabricate a CCTO/PI composite film (with 40 vol. % ceramic filler) with a dielectric permittivity of about 49 at 100 Hz and room temperature, which is approximately 6 times larger than that of pure PI. Babu et al. [23] report the permittivity of CCTO/silicone resin composite is about 13 at 1 kHz and room temperature, which would reach a maximum value by filling with CCTO volume fraction at 50 vol. % and is about 4 times larger than silicone resin. Srivastava et al. [24] also report the dielectric behaviors of CCTO/PVDF composite. The dielectric constant of the CCTO/PVDF composite with 10 wt% of ceramic loading is about 8.2 at 1 Hz and 300 K. However, the grain sizes of CCTO filler of these composites mentioned above are prepared by

*Corresponding author:
Tel : +86-29-62307-012
Fax: +86-29-62307-012
E-mail: zhao1983yang@hotmail.com

several methods that could range from a few to tens of micrometers. In some theoretical models [25], the large dielectric constant of CCTO/polymer dielectric composite may contribute to the morphology and the particle size of the ceramic powder. In addition, the smaller CCTO particles exhibit the larger surface area, which also could influence the dielectric properties. Therefore, ceramic/polymer composite containing different particle sizes of CCTO that exhibit various dielectric properties, and then extraordinary properties of this composite are obtained.

In this study, different sizes of CCTO particles are synthesized by the sol-gel method, and then the composites are fabricated by mixing and mould pressing. These composites, composed of CCTO particles and PF matrix, are studied by varying the filler content and particle size of the fillers. Finally, the variation of dielectric properties of CCTO/PF dielectric composite with certain range of temperature and frequency are measured.

Experimental Methods

Materials

Copper nitrate (99%), calcium nitrate (99%), tetrabutyl titanate ($\geq 98\%$), ethanol ($\geq 99.7\%$), acetic acid ($\geq 99.5\%$), ammonium hydroxide (25%), phenol (99%), formaldehyde (37%), oxalic acid (99.5%) and hexamethylenetetramine ($\geq 99\%$) are purchased from Sinopharm Chemical Reagent Co., Ltd., China. All materials are used without further purifications.

Preparation of CCTO particles

CCTO particle is synthesized by the sol-gel method as follow: copper nitrate, calcium nitrate, and tetrabutyl titanate in the stoichiometric ratio are dissolved ethanol separately. The above solutions are mixed with continual stirring, and then dilute ammonia solution is dripped dropwise into this solution to adjust the pH to 1.0-2.0. The gel is formed at room temperature with several hours. After that the powder is obtained by dried and ground, and then these powder is calcined at 700, 800, 900 °C for 10 h to form the CCTO particles which exhibit different particle size. These particles are abbreviated as CCTO-*i*, CCTO-*ii* and CCTO-*iii*.

Preparation of CCTO/PF dielectric composite

CCTO/PF dielectric composite are prepared by mixing and mould pressing that the material contains different volume of CCTO-*i*, CCTO-*ii* and CCTO-*iii* particles. The CCTO powders are ultrasonically dispersed in mixed solution of phenol and formaldehyde for several hours with stoichiometry $n(\text{C}_6\text{H}_5\text{OH}):n(\text{HCHO}) = 1:0.85$ in order to form a stable suspension. After that, addition of oxalic acid as catalyst, the sample is obtained with polymerization reaction for 3 h at 90 °C. The sample are filtrated, dried at 120 °C in an oven and

then ground into powders. Finally, these powders are well-mixed and molded by hot pressing to obtain the dielectric composite. The final samples with a disk shape are 15 mm in diameter and about 3 mm in thickness. The CCTO/PF dielectric composites with the CCTO-*i*, CCTO-*ii* and CCTO-*iii* particles are named as CCTO-*i* composite, CCTO-*ii* composite and CCTO-*iii* composite respectively.

Characterization techniques

The particle size distributions of CCTO-*i*, CCTO-*ii* and CCTO-*iii* are measured by Laser Particle Size Analyzer. X-ray diffraction patterns are obtained at room temperature with a Cu tube at 40 kV and 100 mA by X-ray diffraction (XRD). The infrared spectra are recorded in the 400-4000 cm^{-1} range by Fourier Transform infrared spectrometer (FTIR). The morphology of composite is examined by scanning electron microscopy (SEM). For electrical measurement, the surfaces of CCTO/PF dielectric composites are sputtered by silver paste to form electrodes. The permittivity and loss tangent of these composites are measured by Agilent 4294A impedance analyzer in a frequency range from 100 Hz to 1 MHz over the temperature range of 25-75 °C.

Results and Discussions

Characterization of CCTO particles

The X-ray diffraction patterns of CCTO particles (CCTO-*i*, CCTO-*ii* and CCTO-*iii*) are shown in Fig. 1(a). The main diffraction peaks of three kinds of CCTO particles are matched to the JCPDS patterns of $\text{CaCu}_3\text{Ti}_4\text{O}_{12}$ for identification [26]. It shows that these particles have a cubic perovskite-related structure (group: Im3). Some minor diffraction peaks of CaTiO_3 , CuO and TiO_2 are detected in these particles, which are consistent with previous literature [27]. CCTO-*i* particles with low calcining temperature exhibit the lower diffraction intensity peak than the CCTO-*iii* particles (the calcine temperature is 900 °C). And the FTIR spectrum of CCTO particle (CCTO-*i*) is shown in Fig. 1(b). A peak appears at 458 and 571 cm^{-1} are attributed to the stretching vibration of Ti-O of CCTO-*i* particles. From the XRD and FTIR, the CCTO particles are successfully prepared by the sol-gel method with different calcine temperatures.

Particle size distribution of CCTO particles (CCTO-*i*, CCTO-*ii* and CCTO-*iii*) is shown in Fig. 2. The Particle size of CCTO powders are prepared by sol-gel method and increased as the calcining temperature rises, and the effective diameter of CCTO particles is a few hundreds of nanometers. The effective diameter is 310 nm for CCTO-*i* particle, which is much lower than the value of 520 nm for CCTO-*iii* particle. CCTO-*i* particle with the lower calcining temperature exhibit small particle size, which due to lower crystallization

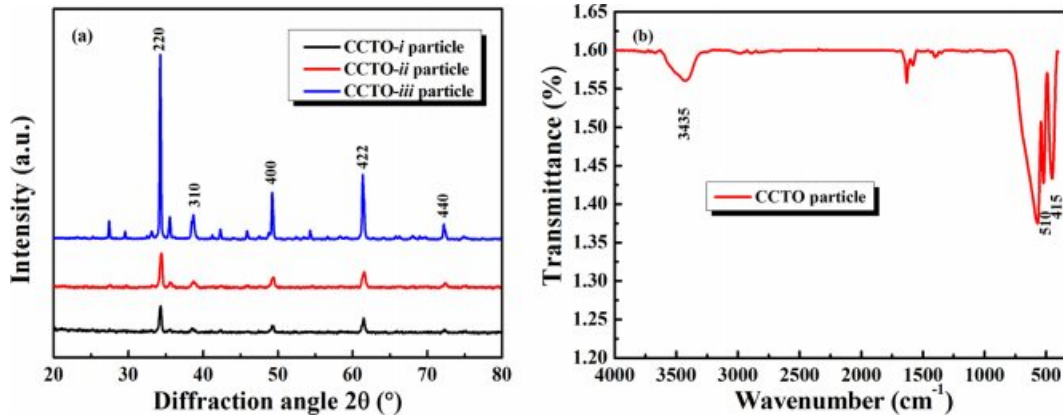


Fig. 1. XRD patterns of CCTO particles (a) and FTIR pattern of CCTO particle (b).

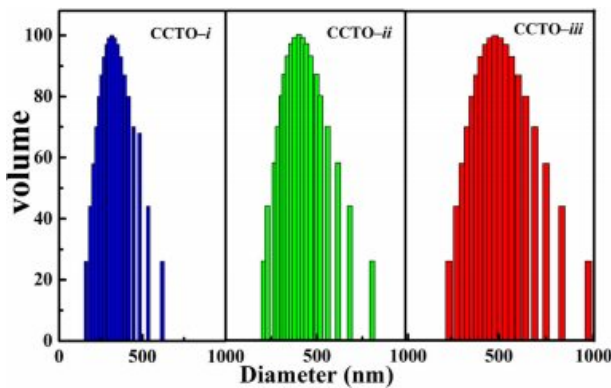


Fig. 2. Particle size distribution of CCTO particles.

temperature. Moreover, the small powder size of CCTO-*i* particle exhibit low diffraction intensity peak, which is consistent with particle size distribution of CCTO-*i* particle.

The structure of CCTO/PF dielectric composites

The FTIR spectra of CCTO/PF dielectric composites with 50 vol. % CCTO-*i* particles, 50 vol. % CCTO-*ii* particles and 50 vol. % CCTO-*iii* particles respectively are shown in Fig. 3. The characteristic peaks at 1101 cm^{-1} and 3384 cm^{-1} are attributed to stretching vibration of C-C and -OH of benzene ring. A peak appears at 1225 cm^{-1} which is attributed to the stretching vibration of -CO-. The characteristic peaks at 458 and 571 cm^{-1} are attributed to the stretching vibration of Ti-O of CCTO particles in spectra a, b and c. The characteristic peaks of C-C, -OH, -CO- and Ti-O become extremely weak in CCTO/PF dielectric composite, which are owing to the fact that the CCTO particles fill in the PF and change the original structure of polymer matrix. These characteristic peaks appear in spectra a, b and c which are an indication that interaction between CCTO and polymer chain to form the CCTO/PF dielectric composite.

Fig. 4 shows the X-ray diffraction pattern of CCTO/PF dielectric composites which contain 50 vol. %

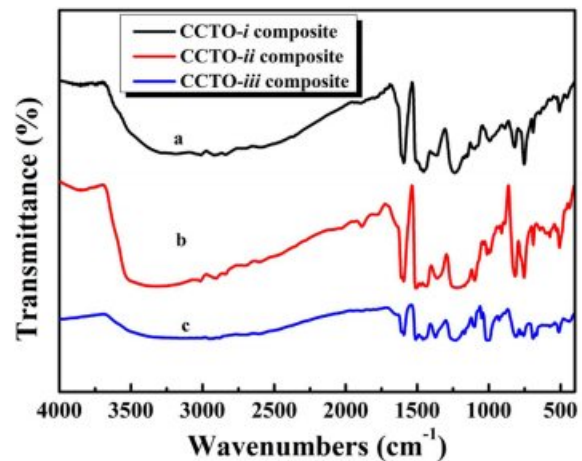


Fig. 3 FTIR spectra of CCTO/PF dielectric composites.

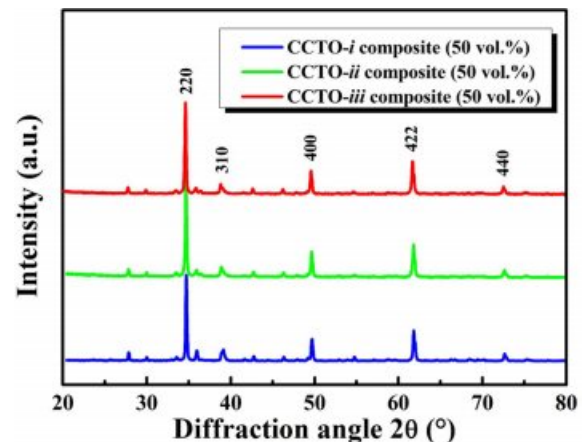


Fig. 4. XRD patterns of CCTO/PF dielectric composites.

CCTO-*i* particles, 50 vol. % CCTO-*ii* particles and 50 vol. % CCTO-*iii* particles respectively. The XRD analysis for three types of CCTO/PF dielectric composites shows the predominance of CCTO phase. It could be seen that all the major diffraction peaks can be indexed as a body centered cubic perovskite-related structure of space group $\text{Im}\bar{3}$ according to JCPDS #75-

2188 and diffraction peak of the PF could not be detected, indicating that CCTO particles dispersed in the PF might have an important effect on the structure of the molecular aggregation of the PF polymer and destroy the ordered structure of the polymer matrix.

To further make clear the morphology of CCTO powders and CCTO/PF composite, SEM images of CCTO-*i* particles and CCTO-*i* composites are presented in Fig. 5(a) and (b) respectively. The result shows that CCTO-*i* particles are in non-spherical shape and with an average diameter of 310 nm, which is in accordance with the results of particle size distribution. Fig. 5(b) shows the surface morphology of CCTO-*i* composites. CCTO particles are homogeneously dispersed in PF matrix to form a composite.

According to the FTIR spectra, X-ray diffraction pattern and SEM image, it would be indicated that CCTO particles disperse into the PF to form a ceramic/polymer dielectric composite.

Dielectric properties of CCTO/PF dielectric composites

Frequency dependences of dielectric constant of CCTO-*i*, CCTO-*ii* and CCTO-*iii* composites at room temperature are shown in Fig. 6(a). It is found that dielectric constant increase gradually with the particle

size of CCTO increase. And in the frequency of 100 Hz to 1 MHz, the decrease in the dielectric constant with increase in frequency is owing to the fact that the dipole orientation polarization and interfacial polarization could not keep up with the alternating field when the frequency is raised. For the CCTO-*i* composite with 50 vol. % ceramic particles, the dielectric constant of this composite is 34.51, which was about 10 times higher than that of pure PF. From the Table 1 it is found that dielectric constant increased gradually with the increase of the content of CCTO, and the permittivity of CCTO-*i* composite with 50 vol. % ceramic particles reach a maximum value, which is much higher than those of CCTO-*ii* composite and CCTO-*iii* composite. Moreover, it could be seen that the CCTO/PF dielectric composites

Table 1. The dielectric constant of CCTO/PF composites on the different fraction of CCTO at 100 Hz and room temperature.

Volume fraction of CCTO	CCTO- <i>i</i> composite	CCTO- <i>ii</i> composite	CCTO- <i>iii</i> composite
10 vol. %	10.95	7.37	6.89
20 vol. %	13.74	9.96	8.7
30 vol. %	18.34	13.67	12.32
40 vol. %	25.66	17.48	15.39
50 vol. %	34.51	27.83	22.91

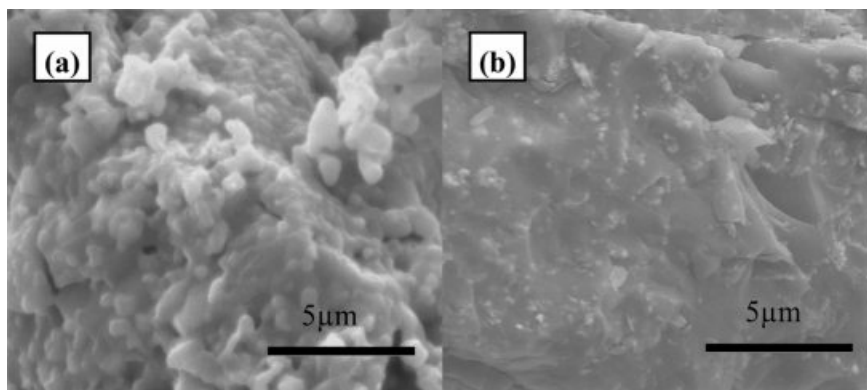


Fig. 5. SEM morphology of the CCTO-*i* particle (a) and SEM image of surface morphology of CCTO-*i* composite with 50 vol. % CCTO particle (b).

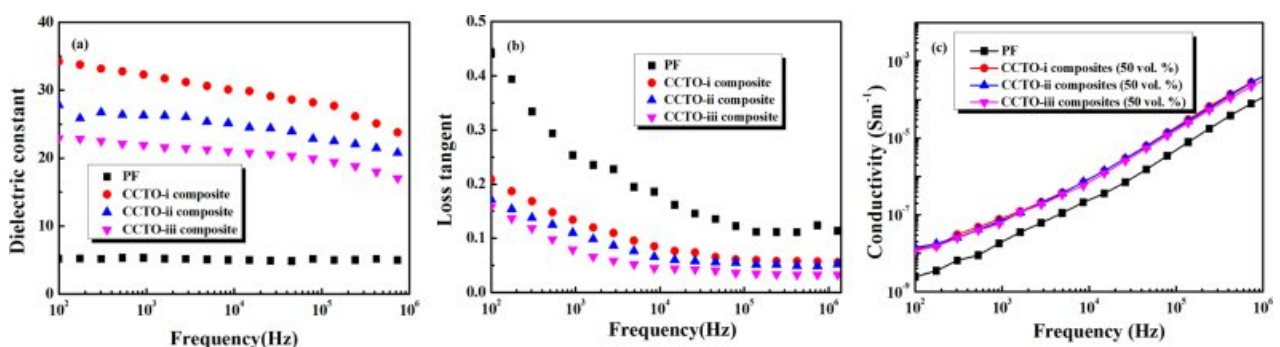


Fig. 6. Frequency dependence of permittivity (a), loss tangent (b) and conductivity (c) of CCTO/PF dielectric composites with 50 vol. % CCTO particle at room temperature.

with three types of particle size are independent in the total range of the measuring frequencies.

The loss tangent of CCTO/PF dielectric composite measured in the frequency range from 100 Hz to 1 MHz at room temperature is shown in Fig. 6(b). With the adding of inorganic filler CCTO, the dielectric loss of three types of composites could be effectively reduced. For the CCTO-*i* composite with 50 vol. % CCTO, the loss tangent decreased to 10^{-2} which was lower than that of polymer matrix (10^{-1}). At the same time, the frequency stability of CCTO/PF dielectric composite is improved by the addition of CCTO. From the Table 2, it is noticed that when volume fraction increase, loss tangent of these composites decrease. This drop of the loss tangent is due to the addition of CCTO to a certain extent which pins the dipole orientation, thus reduced the dielectric loss of composite.

Among the three types of ceramic/polymer dielectric composites, the CCTO-*i* composite with a smaller particle size exhibit excellent dielectric properties that could be influence by different particle sizes. As it could be seen in Fig. 6(c), with the CCTO concentration is 50 vol. %, the conductivity of CCTO-*i* composite is only $10^{-7} \text{ S} \cdot \text{m}^{-1}$ at 100 Hz and room temperature and it increase with an increase in the frequency. It is confirm that insulating layer existed in CCTO/PF dielectric composite and was consistent with the variation of dielectric permittivity.

The temperature dependence of dielectric properties is determined for CCTO/PF dielectric composite.

Table 2. The loss tangent of CCTO/PF composites on the different fraction of CCTO at 100 Hz and room temperature.

Volume fraction of CCTO	CCTO- <i>i</i> composite	CCTO- <i>ii</i> composite	CCTO- <i>iii</i> composite
10 vol. %	0.29	0.27	0.26
20 vol. %	0.25	0.24	0.23
30 vol. %	0.23	0.21	0.21
40 vol. %	0.22	0.18	0.17
50 vol. %	0.21	0.17	0.15

Although the dielectric constant of the CCTO/PF dielectric composites with three types of particles was different, all the composites show the same dependence of the dielectric constant and loss on the temperature. A typical result is shown in Fig. 7, where the temperature dependence of CCTO-*i* composites with 50 vol. % CCTO particles is measured at various frequencies. As shown in Fig. 7, the dielectric constant and loss tangent of the CCTO-*i* composites that containing 50 vol. % CCTO-*i* particles increase slightly with temperature, exhibiting relatively good temperature stability in the measured temperature range from 25 °C to 75 °C at different measured frequencies. Temperature stability of dielectric constant is expressed as $\Delta C_T/C_{25^\circ\text{C}}$ and calculated by the Eq. (1).

$$\frac{\Delta C_T}{C_{25^\circ\text{C}}} = \frac{C_T - C_{25^\circ\text{C}}}{C_{25^\circ\text{C}}} \times 100\% \quad (1)$$

Where $\Delta C_T/C_{25^\circ\text{C}}$ is temperature stability, C is capacitance. The temperature coefficient of CCTO-*i* composite is -3% to 10% from 25 to 75 °C at 100 Hz.

In short, according to the results from the Figs. 6, 7 and Tables 1, 2, we can make a conclusion that the CCTO-*i* composite possess relative high dielectric constant, low loss tangent, as well as the weak frequency and temperature dependence of dielectric constant. From the Table 3, comparing with the existing ceramic/polymer dielectric composites, the dielectric properties of CCTO-*i* composite are comparable to these composites. At the same time, the CCTO-*i* composite is prepared with the small particle size of the ceramic, which could make the CCTO/PF dielectric composite attractive for practical applications.

A mechanism to interpret the variation of dielectric properties of CCTO-*i* composite

In this part, the CCTO-*i* composite is investigated on the variation of dielectric properties that is similar to other composites. Generally, the dielectric properties of

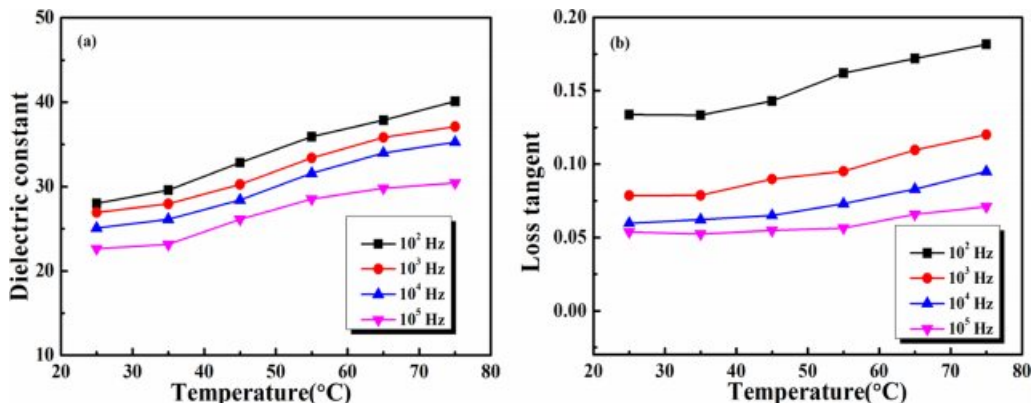
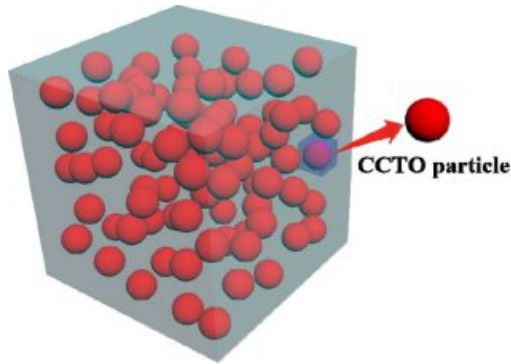


Fig. 7. Temperature dependence of dielectric constant (a) and loss tangent (b) of CCTO-*i* composites with 50 vol. % CCTO particles is measured at various frequencies.

Table 3. Dielectric properties of ceramic/polymer composites at 100 Hz and room temperature.

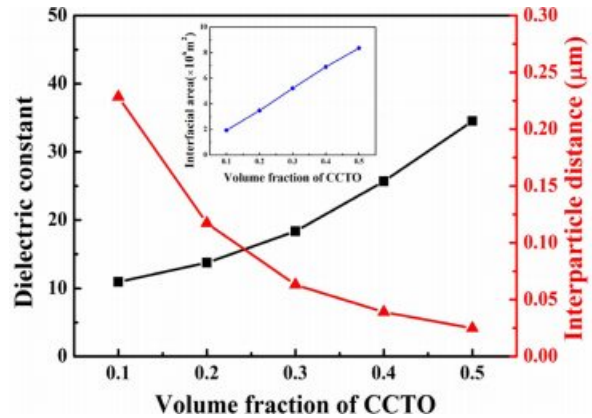
Composite	Dielectric constant	Loss tangent
CCTO- <i>i</i> composites (50 vol. %)	34.51	0.21
(50 vol. %) [21]	32	0.062
(40 vol. %) [22]	50	0.20
CCTO-silicone resin composites (50 vol. %) [23]	15	0.27

**Fig. 8.** An illustration of CCTO particle fills in composite.

CCTO/PF dielectric composite significantly enhance, which attribute to fill the ceramic particles of CCTO with giant dielectric properties. For the CCTO, the high dielectric properties are derived from the specific structure, which is semiconducting grains with insulating grain boundary. High dielectric permittivity of ceramic/polymer dielectric composite originates from internal interfaces effect that may be affected by the variation of interparticle distance and interfacial area [28]. How to calculate the interparticle distance and interfacial area? The assumption is that the ceramic particle is spherical and uniformly distribute in the polymer matrix which is shown in Fig. 8. For another, the interparticle distance of the CCTO/PF dielectric composites is expressed by the equation (2):

$$d = r \left[\left(\frac{4\pi}{3v} \right)^{1/3} - 2 \right] \quad (2)$$

Where d is interparticle distance, r is CCTO particle radius and v is the volume fraction of CCTO particles. And the interfacial area of composites could be calculated in certain volume of the 0-3 type composite (1 m^3). As shown in Fig. 9, with the increase of volume fraction of CCTO-*i* particles, interparticle distance decrease dramatically, and interfacial area, dielectric constant becomes extremely large at the frequency of 100 Hz and room temperature. With the increase the content of ceramic powders, the increase of interfacial area of dielectric is attributed to the reduction of interparticle distance, and then the dielectric constant increase. The results thus clearly suggest that large interfacial polarization mechanisms play a very important

**Fig. 9.** Variation of the interparticle distance, interfacial area (inset) and dielectric constant of CCTO-*i* composites with different volume fraction of CCTO.

role in the dielectric properties of CCTO/PF dielectric composite.

Conclusions

CCTO/PF dielectric composites with three types of CCTO particles have been investigated and discussed. For CCTO-*i* composite containing smaller particle size of CCTO, the dielectric permittivity reach about 34.5 with the volume fraction of CCTO-*i* particle was 0.5 at 100 Hz and room temperature, while remains a low loss tangent about 0.063. The maximum of dielectric constant of CCTO-*i* composite is much larger than that of polymer matrix (PF) and that of other types of CCTO/PF dielectric composites with the same volume fraction. The dielectric properties of CCTO-*i* composite possess relatively high permittivity, as well as exhibit good frequency and temperature stability. And the experimental results show that the large enhancement in dielectric permittivity may attribute to interface effect. It is believed that CCTO/PF dielectric composite with high dielectric permittivity and relatively low loss tangent could be applied in future high-technology fields.

Acknowledgment

This work was supported by the National Natural Science Foundation of China (Grant No. 51673157), the Natural Science Basic Research Plan in Shaanxi Province of China (No. 2017JM5134, No. 2018JM5047

and No.2017JQ2037), Scientific Research Program Funded by Shaanxi Provincial Education Department (Program No. 15JK2188).

References

1. C. Ehrhardt, C. Fettkenhauer, J. Glenneberg, W. Münchgesang, H. S. Leipner, M. Diestelhorst, S. Lemm, H. Beige, and S. G. Ebbinghaus, *J. Mater. Chem. A* 2[7] (2014) 2266-2274.
2. M. N. Feng, X. Huang, H. L. Tang, and X. B. Liu, *Colloids Surf. A* 441[3] (2014) 556-564.
3. K. Brandt, V. Salikov, H. Özcoban, P. Staron, A. Schreyer, L.A.S.A. Prado, K. Schulte, S. Heinrich, and G.A. Schneider, *Compos. Sci. Technol.* 72[1] (2011) 65-71.
4. P. Thomas, R.S.E. Ravindran, and K.B.R. Varma, *J. Therm. Anal. Calorim.* 115[2] (2014) 1311-1319.
5. P. Mishra, P. Kumar, *Ceram. Int.* 41 (2015) 2727-2734.
6. P. Mishra and P. Kumar, *J. Alloys Compd.* 617 (2014) 899-904.
7. M. Mikolajek, A. Friederich, C. Kohler, M. Rosen, A. Rathjen, K. Krüger, and J.R. Binder, *Adv. Eng. Mater.* 17 (2015) 1294-1301.
8. M. Bi, Y. Hao, J. Zhang, M. Lei, and K. Bi, *Nanoscale* 9 (2017) 16386-16395.
9. K. Osińska and D. Czekaj, *J. Therm. Anal. Calorim.* 113 (2013) 69-76.
10. H. Chen, X. Dong, T. Zeng, Z. Zhou, and H. Yang, *Ceram. Int.* 33 (2007) 1369-1374.
11. W. Sun and B. Lu, *Mater. Sci. Eng. B* 127 (2006) 144-149.
12. Z.M. Dang, J.K. Yuan, J.W. Zha, T. Zhou, S.T. Li, and G.H. Hu, *Prog. Polym. Sci.* 57 (2012) 660-723.
13. Y. Rao and C. P. Wong, *J. Appl. Polym. Sci.* 92 (2010) 2228-2231.
14. L.J. Romasanta, P. Leret, L. Casaban, M. Hernández, M.A. de la Rubia, J.F. Fernández, J.M. Kenny, M.A. Lopez-Manchado, and R. Verdejo, *J. Mater. Chem.* 22 (2012) 24705-24712.
15. A.P. Ramirez, M.A. Subramanian, M. Gardel, G. Blumberg, D. Li, T. Vogt, and S.M. Shapiro, *Solid State Commun.* 115 (2000) 217-220.
16. Y. Wang, X. Wu, C. Feng, and Q. Zeng, *Microelectron. Eng.* 154 (2016) 17-21.
17. L. Zhang, X.B. Shan, P.X. Wu, J.L. Song, and Z.Y. Cheng, *Ferroelectrics* 405 (2010) 92-97.
18. Y.C. Qing, W.C. Zhou, F. Luo, and D.M. Zhu, *J. Mater. Chem. C* 1 (2013) 536-541.
19. X. Yang, W. Huang, and Y. Yu, *J. Appl. Polym. Sci.* 120 (2011) 1216-1224.
20. W. Wan, J. R. Luo, C. Huang, J. Yang, Y. B. Feng, W. X. Yuan, Y. J. Ouyang, D. Z. Chen, and T. Qiu, *Ceram. Int.* 44 (2018) 5086-5092.
21. F.J. Wang, D.X. Zhou, and Y.X. Hu, *Phys. Status Solidi A* 206 (2009) 2632-2636.
22. Z.M. Dang, T. Zhou, S.H. Yao, J.K. Yuan, J.W. Zha, H.T. Song, J.Y. Li, Q. Chen, W.T. Yang, and J.B. Bai, *Adv. Mater.* 21 (2009) 2077-2082.
23. S. Babu, K. Singh, and A. Govindan, *Appl. Phys. A* 107 (2012) 697-700.
24. A. Srivastava, K. K. Jana, P. Maiti, D. Kumar, and O. Parkash, *Mater. Res. Bull.* 70 (2014) 735-742.
25. B.C. Luo, X.H. Wang, Y.P. Wang, and L.T. Li, *J. Mater. Chem. A* 2 (2014) 510-519.
26. S. Jesurani, S. Kanagesan, and K. Ashok, *J. Sol-Gel Sci. Technol.* 64 (2012) 335-341.
27. C. Yang, H.S. Song, and D.B. Liu, *Composites Part B* 50 (2013) 180-186.
28. Y. Yang, B.P. Zhu, Z.H. Lu, Z.Y. Wang, C.L. Fei, D. Yin, R. Xiong, J. Shi, Q.G. Chi, and Q.Q. Lei, *Appl. Phys. Lett.* 102[4] (2013) 042904.